1993

Nondestructive Characterizations of Polyethylene/Nylon Laminates by Near-Infrared Spectroscopy

Charles E. Miller
Haverford College

Svend A. Svensden

Tormod Naes

Nondestructive Characterizations of Polyethylene/Nylon Laminates by Near-Infrared Spectroscopy

CHARLES E. MILLER,* SVEND A. SVENDSEN, and TORMOD NÆS
MATFORSK, Norwegian Food Research Institute, Osloveien 1, N-1430 Aas, Norway

The use of near-infrared (NIR) spectroscopy for the rapid and nondestructive analysis of food packaging laminates containing polyethylene (PE), polyamide-6 (PA-6), and ethylene vinyl alcohol (EVOH) layers is demonstrated. The method of Pathlength Correction with Chemical Modeling (PLC-MC) is used to estimate the total laminate thickness, and Principal Component Regression (PCR), is used to estimate the thickness percentages of PE and EVOH in the laminates, from NIR reflective-transmission spectra in the region 1500-2500 nm. Results indicate that the NIR method can be used to determine the total laminate thickness within 2-4 μm, the PE layer thickness percentage within 0.7-1.8%, and the EVOH layer thickness within 0.7-0.8 μm. In addition, detailed observation of the PCR models indicates that the NIR method is also sensitive to the absorbed water content, the morphology of the polymers, and perhaps the amount of polyurethane adhesive in the laminates. The usefulness of PCR outlier detection, for identification and characterization of strange samples, and principal component rotation, for improvement of PCR model interpretability, is also demonstrated.

Index Headings: **Near-infrared; Polymers; Laminates; Principal component regression.**

INTRODUCTION

Polymeric materials are particularly useful for food packaging applications, because they are relatively cheap and can provide the necessary physical and chemical properties. The use of layered polymer film structures, or laminates, has been common for packaging applications, because such materials can be easily designed to possess a wide range of food protection qualities (such as oxygen, water, and CO_2 resistance, and physical strength).[1-5]

The relative amounts of different layers in a laminate, the microstructure of the polymers in each layer, and the concentrations of additives or contaminants greatly influence the food protection qualities of a laminate. As a result, a nondestructive method that can determine such properties would be very useful for product quality assessment. In addition, rapid and nondestructive determinations of properties during laminate production would be particularly useful for process monitoring and control purposes. Near-infrared (NIR) spectroscopy is one example of a rapid and nondestructive method and has demonstrated its ability to determine compositional and structural properties of bulk polymers[6] and polymer films.[7-9]

The purpose of this work is to demonstrate the ability of NIR spectroscopy, combined with multivariate modeling methods, to rapidly and nondestructively estimate quality parameters of polymeric laminates that are used extensively in the food industry. For this purpose, a polyethylene/polyamide-6/ethylene vinyl alcohol (PE/PA-6/EVOH) laminate, which is used for the packaging of meat and cheese,[10] is used. The ability of the NIR method to determine three different properties of the laminate—total thickness, thickness percentage of polyethylene, and thickness percentage of ethylene vinyl alcohol—is addressed. In addition, the sensitivity of the NIR method to other parameters, such as the amount of absorbed water, the amount of adhesive, and the morphology of polymers in the laminate, is discussed.

THEORY

The data analysis techniques that were used to provide information from NIR spectra have been described previously.[11-17] However, a short overview of these methods is provided, along with more detailed discussions regarding the specific aspects of these methods that are useful for our analysis.

Principal Component Regression. Principal Component Regression[11] is a linear multivariate method that can be used to construct a calibration between NIR spectral intensities (or variables) and a property of interest. Construction of a PCR model involves the decomposition of the NIR spectral data for a set of calibration samples (contained in matrix **X**) into a few principal components of variation, according to the model:

$$\mathbf{X} = \mathbf{T}\mathbf{P}^t + \mathbf{E} \quad (1)$$

where **T** represents the source of each sample for each principal component, **P** represents the loadings of each NIR spectral variable for each principal component, and **E** is the model "error." Given **X**, **T** and **P** are determined by an iterative procedure. At this point, a model relating the principal components (or "reduced" NIR variables, **T**) to the property of interest (**y**), measured by a reference method, can be constructed:

$$\mathbf{y} = \mathbf{T}\mathbf{q} + \mathbf{f} \quad (2)$$

where **q** contains regression coefficients, and **f** is the modeling error. Given **T** and **y**, **q** is estimated by least-squares. Once the PCR model (defined by **P** and **q**) is determined, the property of a future sample (y_s) can be estimated from its NIR spectrum ($\mathbf{x}_s$):

$$y_s = \mathbf{x}_s\mathbf{P}\mathbf{q}. \quad (3)$$

During the construction of a PCR model, it is necessary to perform a validation procedure in order to determine the optimal number of principal components for the model and to estimate the prediction performance of the model. There are several validation procedures that can be used for this purpose,[18] including leverage correction,

Received 20 July 1992.
* Author to whom correspondence should be sent. Present address: DuPont Polymers, Industrial Polymers Research, P.O. Box 1089, Bldg. 10, Orange, TX 77631-1089.

0003-7028/93/4703-0346$2.00/0

cross-validation, and the use of an independent test set of samples.

Although the primary purpose of PCR modeling is to enable prediction of the property of interest of a future sample from its NIR spectrum, additional information can be obtained. For example, the detection of an outlier sample during future predictions can be made from observation of the spectral residual of this sample. The spectral residual for any sample ($\mathbf{e}_s$) is the part of the sample's spectrum ($\mathbf{x}_s$) that cannot be modeled by the calibration:

$$\mathbf{e}_s = \mathbf{x}_s - \hat{\mathbf{x}}_s = \mathbf{x}_s - \mathbf{x}_s\mathbf{P}\mathbf{P}^t \quad (4)$$

where $\hat{\mathbf{x}}_s$ ($= \mathbf{x}_s\mathbf{P}\mathbf{P}^t$) is the best possible reconstruction of the sample's spectrum, with the use of the PCR model. A test set sample is an "outlier" if the magnitude of $\mathbf{e}_s$ for that sample is much larger than the magnitudes of the various $\mathbf{e}_s$ spectral residuals obtained with the use of calibration sample spectra. In addition, $\mathbf{e}_s$ has the same dimensionality as a spectrum, and can thus be interpreted like a spectrum, in order to determine the cause of the sample's uniqueness. It should be noted that the PCR method provides other means of outlier detection, for example, by leverage and influence measures.[19] Outlier detection is an advantage shared by many full-spectrum calibration techniques, including PCR and Partial Least-Squares (PLS).[20]

A second additional feature of the PCR method is the ability to gain information regarding interferences with the determinations of the property of interest, through observation of the PCR model scores ($\mathbf{T}$) and loadings ($\mathbf{P}$). The scores, which indicate relationships between samples, can be used to determine whether the NIR method can detect known, designed trends in the samples. The loadings indicate the nature of the sensitivity of the NIR spectrum to properties that vary in the samples, and thus can be used to identify the means by which the NIR method measures a known property of the samples, or to discover the sensitivity of the NIR method to an unknown property of the samples. Each PCR loading has the same dimensionality as a spectrum, and can be interpreted like a spectrum. However, because loadings describe *variations* in properties, rather than absolute concentrations of constituents, it is often better to interpret them as difference spectra. These interpretations are significantly aided by the use of model compound spectra, such as the spectra of pure constituents, or the spectra of a single constituent in two different structural states. However, it should be noted that no principal component ever describes the variation in only one property at a time, and therefore each principal component loading might simultaneously describe the variations of several different properties. Fortunately, such poor interpretability of the principal components can in some cases be improved through the use of rotation, which is described below.

Rotation of Principal Components. In the case that the samples used in the PCR modeling have known or designed variations, and that each principal component is observed to describe several of these known variations simultaneously, the components can be rotated so that each of them corresponds more exclusively to one of the known variations in the samples. The purpose of such a rotation is to obtain a better understanding of the NIR sensitivity to the known properties through the observation of the rotated component loadings.

Simultaneous rotation of two principal components can be done according to Eq. 5:

$$\mathbf{P}_{2,\text{rot}} = \mathbf{P}_2 \cdot \begin{pmatrix} \cos\theta & -\sin\theta \\ \sin\theta & \cos\theta \end{pmatrix} \quad (5)$$

where $\mathbf{P}_2$ contains two of the principal component loadings obtained from the original PCR model (Eq. 1), θ is the rotation angle, and $\mathbf{P}_{2,\text{rot}}$ are the rotated versions of the two component loadings. At this point, the corresponding rotated scores ($\mathbf{T}_{2,\text{rot}}$) can be determined:

$$\mathbf{T}_{2,\text{rot}} = \mathbf{X}\mathbf{P}_{2,\text{rot}}. \quad (6)$$

Different rotations at different angles (θ) are done until the PCR scores ($\mathbf{T}_{2,\text{rot}}$) of each of the two principal components correlate more closely to known sample variations. At this point, the loadings for the two rotated components can be interpreted to provide better information regarding the sensitivity of the NIR method to these known variations. Similar rotation procedures have been used previously[12,13] to improve the interpretability of the results of principal component analysis.

Total Laminate Thickness Determinations. If one assumes that the Beer–Lambert law is a valid approximation for the spectral measurements performed in this study, the total laminate thickness is expected to have a purely multiplicative effect on the NIR spectrum. Therefore, it is necessary to use a multiplicative model to relate the NIR spectrum to the total thickness. In this work, two different multiplicative models for total thickness estimation are used: (1) the Multiplicative Signal Correction (MSC) model[14,15] and (2) the Pathlength Correction with Chemical Modeling (PLC-MC) model.[16] A theoretical and experimental comparison of these two methods is given in Ref. 16.

In practical usage, a total thickness model is constructed with the use of calibration set spectra that are normalized to represent a single "reference" total thickness, and the model is then used to estimate the total thickness of future test set samples from their non-normalized spectra. It should be mentioned that if a linear model (such as a PCR model) is to be constructed from the same spectral data that are analyzed by the total thickness model, it would be ideal to use the same total thickness-normalized training set spectra for the linear modeling and estimated total thickness-normalized spectra for prediction. Such use of prior information before linear NIR modeling[17] is expected to result in reduced complexity, and thus improved interpretability, of the linear model.

The following discussion of the total thickness estimation methods pertains to spectral data that contain no additive (i.e., baseline offset) variations.

MSC Method. The MSC model, as used in this work, is given by Eq. 7:

$$\mathbf{x}_s = a_{msc}\mathbf{x}_m + \mathbf{e} \quad (7)$$

where $\mathbf{x}_s$ is an individual sample spectrum, $\mathbf{x}_m$ is a "reference" spectrum (often the average spectrum of the calibration set), and a_{msc} is the multiplicative coefficient.

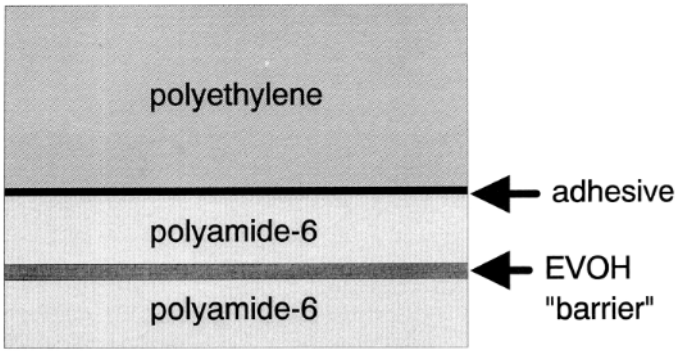

FIG. 1. Layer structure of the laminates used in this work.

Given a sample spectrum ($\mathbf{x}_s$), and a reference spectrum ($\mathbf{x}_m$), a_{msc} is estimated by a least-squares procedure. It is the estimated parameter, a_{msc}, that is proportional to the thickness of the sample represented by $\mathbf{x}_s$. The advantage of this method is that it requires only the selection of an appropriate "reference" spectrum ($\mathbf{x}_m$) for total thickness estimation, and thus does not require a separate training set to execute. However, this method neglects the effect of chemically based spectral variations during the estimation of the total thickness. This assumption is inaccurate, and thus causes the MSC method to provide inaccurate total thickness predictions, if chemically based variations in the spectra are large.[16]

It should be mentioned that there is a more general form of the MSC model,[14,17] which takes into account both additive and multiplicative effects in the spectra. However, the MSC method described by Eq. 7 is used in this work to enable a more direct comparison with the PLC-MC method (which does not take into account additive spectral variations, as discussed below).

PLC-MC Method. In contrast to the MSC model (Eq. 7), the PLC-MC model is:

$$\mathbf{x}_s = (a_{plc}/a_r)\mathbf{x}_m + (a_{plc}/a_r)\mathbf{t}_s\mathbf{P}^t + \mathbf{e} \qquad (8)$$

where a_r is an arbitrary reference total thickness; $\mathbf{P}$ are the loadings of the principal components obtained from a principal components decomposition (according to Eq. 1) of the training set spectra that are normalized to the reference total thickness; $\mathbf{t}_s$ are the scores of the test set sample if its total thickness is equal to the reference thickness; and a_{plc} is the total thickness of the test set sample. Given a_r, $\mathbf{x}_p$, $\mathbf{x}_m$, and $\mathbf{P}$, $(a_{plc}/a_r)\mathbf{t}_s$ and (a_{plc}/a_r) are estimated by least-squares, thus yielding the estimated thickness (a_{plc}) of the test set sample.

In practice, the normalized training set spectra can be obtained in two different ways: (1) careful preparation of training set samples that each have a total thickness equal to a_r, or (2) mathematical normalization of the training set spectra, with the use of experimentally measured total thickness values. The optimal number of principal components used in the PLC-MC correction can be determined by cross-validation or leverage correction.

For the laminate samples used in this work, it was found that the mean calibration spectrum $\mathbf{x}_m$ and the loading for the first principal component obtained from the mean-centered calibration sample spectra (in $\mathbf{P}$) were highly colinear. This situation, as previously expected,[17] resulted in unstable least-squares estimations. Therefore, the PLC-MC model was modified to solve this problem:

$$\mathbf{x}_s = (a_{plc}/a_r)\mathbf{t}_{s,n}\mathbf{P}_n^t + \mathbf{e} \qquad (9)$$

where $\mathbf{P}_n$ are the loadings of the principal components obtained from a principal components decomposition of the total thickness-normalized, but *not* mean-centered, training set spectra. The least-squares-determined parameter for each test set sample is, in this case, $(a_{plc}/a_r)\mathbf{t}_{s,n}$, where $\mathbf{t}_{s,n}$ are the scores that would be obtained if the test set sample had a total thickness equal to the reference thickness. In order to determine the total thickness (a_{plc}) from $(a_{plc}/a_r)\mathbf{t}_{s,n}$, a second model, relating the PCA scores to the pathlength, needs to be constructed:

$$\mathbf{T}_n\mathbf{k} = \mathbf{1}a_r \qquad (10)$$

where $\mathbf{T}_n$ are the scores obtained from the principal components decomposition (according to Eq. 1) of the normalized training set spectra, and $\mathbf{1}$ is a vector of ones. Once the least-squares estimated coefficients $\mathbf{k}$ are determined, the model in Eq. 10 is used to determine a_{plc} from $(a_{plc}/a_r)\mathbf{t}_{s,n}$:

$$(a_{plc}/a_r)\mathbf{t}_{s,n}\mathbf{k} = (a_{plc}/a_r)(1 \cdot a_r) = a_{plc}. \qquad (11)$$

The advantage of the PLC-MC method is that it accounts for chemically based variations in the spectra during the estimation of the total thickness, and is therefore more accurate than the MSC method if such spectral variations are large. The disadvantages of this method are that principal component decomposition must be done (therefore causing the method to be more time consuming) and that total thickness-normalized training set spectra must be obtained (which can be experimentally difficult in some cases).

EXPERIMENTAL

Materials. Two different sets of materials were used for this work: (1) a set of PE/PA-6/EVOH laminates (with the layer structure shown in Fig. 1), which had known variations in the total thickness and polyethylene thickness percentage (PE%), and (2) a set of co-extruded films of PA-6 and EVOH (hereby referred to as NEN films, which have the same structure as the laminate, but without the PE layer), which had known variations in the EVOH thickness percentage (EVOH%). The laminate samples were used to test the ability of the NIR method to determine total laminate thickness and PE%, and the NEN samples were used to test the ability of the method to determine the EVOH%.

Laminates. A series of eight different commercial Riloten-X laminates (Otto Nielsen Emballage AS, DK-2800 Lyngby, Denmark) were used for the laminate studies. These samples were produced by laminating a NEN film to a low-density polyethylene layer, with the use of polyurethane adhesive. The samples were supplied as rolls (ranging from 25 to 50 cm wide) containing approximately 5 to 10 meters of laminate. For each sample roll, four replicate NIR samples were cut (as circles of 3.5 cm diameter) approximately 10 to 20 cm from each other along the roll.

Reference measurements of the thicknesses of the

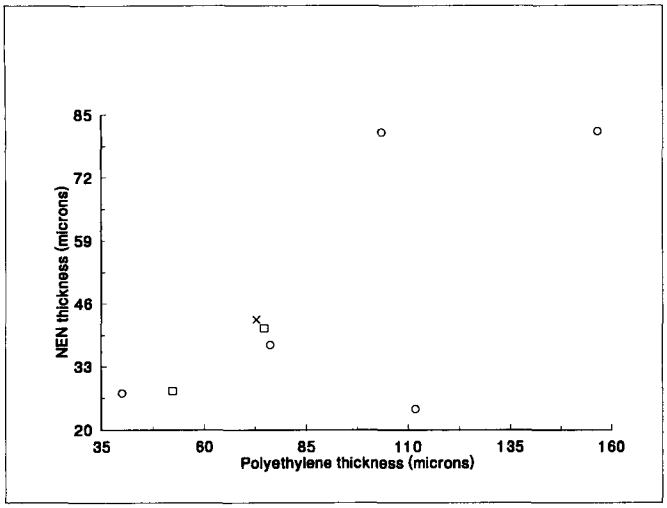

FIG. 2. Design of the samples used in the laminate analyses, in terms of their polyethylene and NEN thicknesses: (○) calibration sample; (□) test set sample; and (X) known outlier sample.

polyethylene (PE), polyamide-6 (PA-6), and ethylene vinyl alcohol (EVOH) layers in all of the laminate samples were obtained by polarized light microscopy of a single cross-sectional cut obtained from each sample roll. Figure 2 shows the distribution of the microscope-determined thicknesses of the PE and NEN layers in the laminate samples. Of the eight different laminates, five were selected for the calibration set and three were used as an independent test set (as shown in Fig. 2). These samples were selected in such a way that the calibration set covered the full range of total thickness and PE% values and the prediction set contained samples with total thickness and PE% values within the ranges of the calibration set. One of the three test set samples was designated a "known" outlier sample, because it was known to contain a unique quality of polyethylene. Although the design of the samples is very limited by availability, it is certainly adequate to demonstrate the basic ability of the NIR method to determine the total thickness and PE%.

NEN Films. The laminate samples did not have sufficient variation in their EVOH% values to enable an evaluation of the NIR method for the determination of this property. Therefore, NEN film samples with wide variations in the EVOH% were used for this purpose. A single NEN co-extruded sheet (approximately 120 μm thick, 25 cm wide, and 120 cm long) was supplied by Otto Nielsen Emballage AS (Lyngby, Denmark). Because the thicknesses of the EVOH layers are known to vary along the long axis of such a sheet (corresponding to the direction of travel of the film out of the extruder), sixteen NIR samples were cut from different spatial regions along the long axis of the sheet. After the NIR analyses, the relative thicknesses of the EVOH and polyamide-6 layers in each of the NIR samples were obtained by polarized light microscopy of a cross-sectional cut taken from the middle section of the NIR sample.

Model Compounds. Films of the pure PA-6, EVOH, and PE used in the laminates were hot-pressed in a vacuum (about 5×10^{-3} mbar) at approximately 240, 210, and 200°C, respectively, with the use of a manual press apparatus attached to a vacuum line and a silicone oil bath (temperature-controlled to within 5°C). In addition, an adhesive sample was prepared by applying a thin layer of the solvent-based adhesive to the gold-reflecting surface of the NIR reflectance cell and allowing the adhesive to cure. Annealing of the NEN, PA-6, and EVOH samples was done at 145–155°C for 30 min in a vacuum of approximately 5×10^{-3} mbar. The spectra obtained from these model experiments were used to aid interpretation of the PCR calibration models.

NIR Spectroscopy. A Technicon InfraAlyzer 500C NIR reflectance spectrometer was used to obtain the NIR spectra. Each NIR sample was prepared by "sandwiching" the film between a gold-reflecting background and a glass cover window. NIR spectra were then collected in reflective transmission mode. For the laminate samples, the PE side of the laminate was always in contact with the gold-reflecting surface. The empty gold background reflectance cell was used as a reference sample. NIR spectral absorbances were obtained over the region 1100 to 2500 nm in 2-nm increments.

Polarized Light Microscopy. Samples for light microscopy measurements were prepared by making a cross-sectional cut (20 μm × 10 mm) of the laminate, with the use of a microtome. The small piece was then mounted onto a microscope glass slide with a cover. The sample was then viewed at 40× magnification with a light microscope equipped with two polarizers (Jenamed 2, Carl Zeiss). For each sample, the polarizers were set so that a large color contrast between the different layers in the laminate was obtained. A scale mounted in the microscope was used to determine the thicknesses of the layers in the laminate.

Data Analysis. *Laminate Samples.* Each NIR spectrum was background-corrected by subtracting the spectrum of the empty gold background reflectance cell from the sample spectrum. Then, every two consecutive intensity points in each of the spectra were averaged, in order to reduce the number of data points. An arbitrary baseline correction was then performed by subtracting the intensity in each spectrum by the intensity at 1640 nm (which corresponded to the minimum spectral intensity for most of the samples).

Two different spectral sub-ranges were used for analysis: 1500–2500 nm and 1600–2240 nm. The 1500–2500 nm range contains first-overtone CH bands and combination bands involving CH, NH, and OH groups, which have absorptivities that are suitable for the sample thicknesses used in this work. The 1600–2240 nm subregion excludes the strong methylene combination bands at approximately 2310 nm and 2350 nm, which (as discussed later) were too strong for accurate quantitative analyses of the thicker laminate samples.

A flow diagram of the calibration and prediction procedures regarding the laminate samples is shown in Fig. 3. Regarding the calibration procedures, the spectrum of each calibration sample was first normalized to its measured total thickness, and then mean-centered before PCR modeling. A PCR calibration model relating the NIR data to PE% was then constructed, and the optimal number of principal components in the model was determined by leverage correction.[18] The chosen optimal number of principal components for the model was the number at which the addition of another principal com-

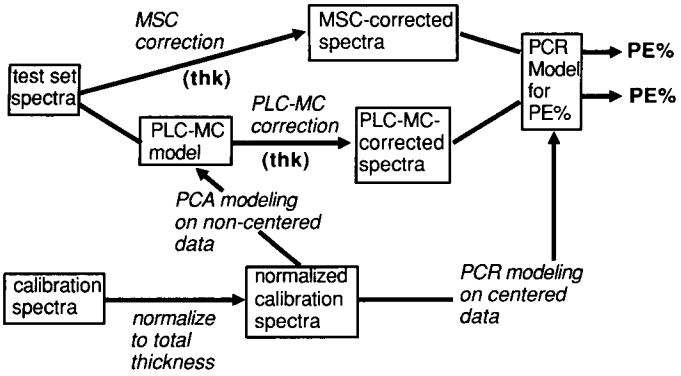

FIG. 3. Flow diagram indicating the calibration and test set prediction procedure for the laminate samples. Entries in boldface indicate parameters that are estimated during a specific step (**thk** = total laminate thickness).

ponent did not "significantly" decrease the leverage-corrected prediction error for PE%.

Regarding the prediction procedure, the total thicknesses of the test set samples were estimated from their spectra with the use of either the MSC or PLC-MC method. Regarding the PLC-MC correction, a principal component analysis of the non-mean-centered, but total thickness-normalized, NIR calibration sample spectra was used to calibrate the correction method (i.e., determine $\mathbf{P}_n$ in Eq. 9), and the total number of principal components used in the PLC-MC correction was determined by leverage correction. The PLC-MC method required the use of four principal components for the 1600–2240 nm region and five principal components for the 1500–2500 nm region. After the total thickness of a test set sample was estimated (either by MSC or by PLC-MC), its spectrum was normalized to the estimated total thickness, mean-centered, and used with the PCR calibration model for PE% to compute estimated PE% values. PCR and PCA analyses were done with the use of the Unscrambler software package (CAMO A/S, Trondheim, Norway).

Calibration errors (RMSEE = root mean square error of estimation) for PE% are expressed as the root mean square of the differences between the measured values and the values estimated by the model from the spectra, for only the calibration samples. Prediction errors (RMSEP = root mean square error of prediction), for both PE% and total thickness, are expressed as the root mean square of the differences between the measured values and the values estimated by the model, for the test set samples only.

NEN Samples. All 501 of the NIR wavelength responses in the range 1500 to 2500 nm (at 2-nm intervals) were used in the EVOH thickness study. The method of Multiplicative Signal Correction (MSC)[14,15] was used to reduce the effects of baseline offset and multiplicative pathlength variations in the spectra of the samples. A PCR model was then constructed with the use of mean-centered spectra and the thickness percentages of the EVOH layers (EVOH%) in the samples, as determined by polarized light microscopy. The calibration error is expressed as the RMSEE (defined above).

Two separate cross-validation analyses were performed in order to estimate the prediction error and the optimal number of principal components in the PCR model. In each case, the validation set contained six samples that had well-distributed EVOH% values, and excluded the samples with the highest and lowest EVOH% values. For each validation, the EVOH% values of the six validation samples were predicted by a PCR calibration that was constructed with the remaining ten samples. The validation error reported is the average of the two RMSEP values obtained when the EVOH% values of the two different validation sets were predicted. The optimal number of principal components in the model was chosen as the number at which the addition of another principal component did not "significantly" decrease the average validation error for the two validation sets.

After the PCR model was constructed, it was found that a rotation of the first two principal components by $\theta = 30°$ (see Eq. 5) was necessary to improve the interpretability of the model. This optimal rotation angle was determined solely from visual observation of the scores, and knowledge of the EVOH% values of the samples.

RESULTS AND DISCUSSION

Calibration and Prediction Statistics. *Laminate Analysis.* Table I shows the calibration, validation, and test set prediction statistics for both the total laminate thickness and the PE% analyses. Validation results for the PCR calibrations indicate that five principal components are required to explain the variation in the spectra in the 1500–2500 nm region, but only four principal components are required for the 1600–2240 nm region. Although the use of four or five principal components in a calibration model constructed from five chemically different samples (Fig. 2) might appear to indicate overfitting, it should be restated that four replicates of each sample were used for the calibration analyses. Further-

TABLE I. Calibration and prediction statistics for laminate analyses.

	Calibration			Prediction			
				RMSEP thickness (μm)		RMSEP PE%	
Spectral region used (nm)	RMSEE (PE%)	Optimal number of PCs[a]	Total thickness estimation method	Test set	Known outlier	Test set	Known outlier
1500–2500	0.75	5	PLC-MC	2.57	4.78	1.43	1.86
			MSC	2.75	1.91	1.34	2.62
1600–2240	0.99	4	PLC-MC	2.36	6.99	0.74	2.62
			MSC	4.17	4.18	0.96	5.09

[a] Determined by leverage correction; PCs = principal components.

TABLE II. PCR calibration and validation results: thickness percentage of EVOH in NEN films.

Optimal number of PCs[a]	2
Calibration error (RMSEE)	0.41% (approx. 0.49 μm)
Validation error (RMSEP)	0.52% (approx. 0.62 μm)
Range of EVOH% values	3.11–8.09% (3.75–9.50 μm)

[a] Determined with the use of two manually selected validation sets; PCs = principal components.

more, interpretation of the PCR model for the calibration that uses the 1600–2240 nm region (discussed later) reveals that only one of the four principal components in the model corresponds to variations between samples with different PE% values, and the other principal components describe different variations between replicates. Therefore, we feel that the use of four and five principal components in the PCR calibrations is justified.

It is interesting to note that the less-complex models that use the narrower 1600–2240 nm region provide consistently better test set predictions for both total thickness and PE% than the more complex five-principal-component models that use the wider 1500–2500 nm range. Inspection of the PCR model obtained from the wider wavelength range indicates that this discrepancy is most likely caused by nonlinearity of the strong $-CH_2-$ bands at 2310 and 2350 nm. Because these absorbances are very strong for the thicker laminate samples, stray light becomes significant in comparison to the light reflected from the samples at these wavelengths, thus resulting in a nonlinear spectral response to layer thickness. However, the PCR calibration method was able to model this interference in the 1500–2500 nm region, and thus perform comparable, although not optimal, predictions.

Test set prediction errors for PE% range from 0.74 to 1.43%, and the prediction errors for total thickness range from 2 to 4 μm. Prediction errors for the known outlier sample are, as expected, significantly greater than for the test set samples. Because the design of the laminate samples used in this work was limited, it should be stressed that these statistics indicate approximate prediction performances of the NIR method. However, it should be noted that detailed interpretations of the PCR model loadings and scores (discussed later) show that the NIR method indeed has the expected spectral sensitivity to PE%. In further support of the NIR method, an additional computation was performed with a different set of five calibration samples and two test set samples (one of which had to be an extreme sample in the design, due to the limited number of samples). Although this computation resulted in expectedly higher prediction errors, it still indicated the basic feasibility of the NIR method.

Comparison of the two sets of results obtained from the different total thickness estimation methods indicates that the PLC-MC method performs similarly to, or slightly better than, the MSC method. The PLC-MC method has the extra ability to account for chemically based spectral variations that constitute a deviation from the average calibration sample (this is clearly observed if the model for the MSC method, Eq. 7, is compared to the model for the PLC-MC method, Eq. 8). Therefore, the comparable performances of the PLC-MC and MSC methods in this case might be caused by the fact that the PE% values for the test set samples (64.6% and 65.1%) are very close to the mean of the values for the calibration samples (66.0%).

EVOH Thickness Determination. Table II shows the results of calibration and validation analyses, regarding EVOH% determination. Results of validation analyses indicate that the use of two principal components was sufficient to model the variation in the NIR spectra of the NEN co-extruded film samples. It was also determined by validation analysis that the NIR method can predict the EVOH% in these films within an error of 0.52%. In terms of EVOH layer thickness, this error translates to 0.62 μm, if it is considered that each of the samples has a total thickness of 120 μm. Although this error might be adequate for analyses of thicker films, it might be inadequate for analyses of thinner films, in which the EVOH thicknesses can approach 1 to 2 μm. However, these results demonstrate the basic usefulness of the NIR method for the determination of the EVOH% in thicker NEN films for both co-extrusion process control and final laminate product quality analysis.

Regarding NIR transmission and reflective transmission analyses of NE films, it was often found that significant interference fringes were present in the spectra, especially in the spectra of films that are thinner than 80 μm. Such fringes, presumably caused by the lack of surface roughness and high optical transparency of the films, pose a significant interference problem for transmission spectroscopic analyses of thin NEN extrudates. Such interferences can be modeled by multivariate calibration methods (such as PCR), but usually not without a decrease in prediction performance. As a result, the use of alternative NIR spectral measurement strategies[21,22] or other spectral methods, such as IR-attenuated total reflectance or NIR-Raman spectroscopy, could result in improved precision for analyses of NEN films that are thinner than 80 μm.

Outlier Sample Analysis. Successful detection and characterization of outlier samples is of particular importance in quality assessment. In this case, the "known outlier" sample is known to have significantly different food protection qualities than the other samples used in this analysis. As mentioned earlier, and shown in Table I, the predictions of total thickness and PE% for the known outlier sample were consistently worse than for the normal test set samples. However, this result might only indicate that the reference thickness values for this sample were inaccurate. The fact that this sample is indeed chemically unique is indicated by observation of its spectral residual (Eq. 4), compared to the average (over replicates) of the spectral residuals for the calibration samples (Fig. 4). The unusually high magnitude of the spectral residual for the known outlier sample indicates that this sample has unique spectral information that the calibration samples lack.

After the known outlier sample was correctly identified, more specific information regarding its uniqueness was obtained by spectral interpretation of its residual. Comparison of this residual to the difference spectrum of [EVOH − PA-6] (Fig. 5) reveals some striking similarities. The strongest similarity involves the strong positive band at approximately 2090 nm, which is most likely an -OH combination band from the EVOH. This result

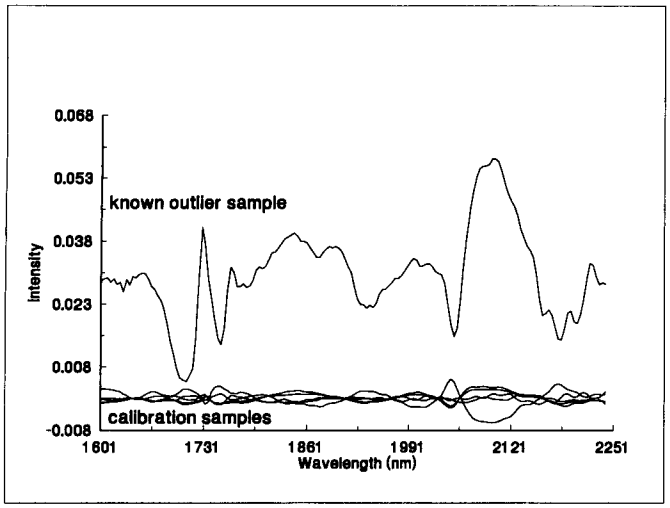

FIG. 4. Comparison of the average spectral residual of prediction for the known outlier sample with the average spectral residuals for the calibration samples.

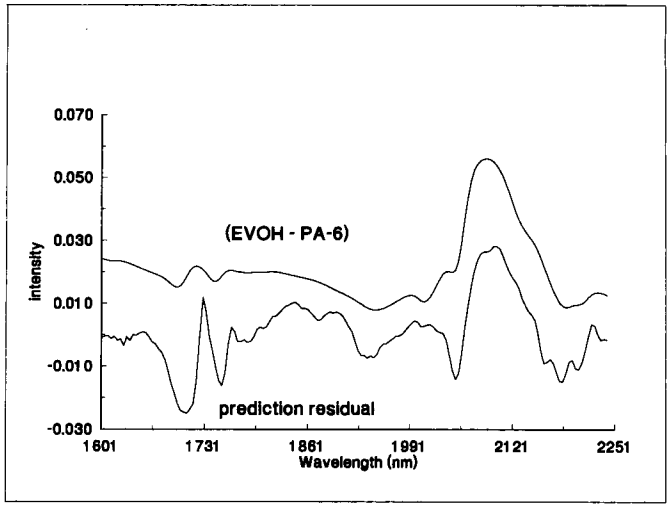

FIG. 5. Comparison of the average spectral residual of prediction for the known outlier sample with the subtraction spectrum of [pure EVOH − pure PA-6]. The subtraction spectrum is scaled for clarity.

suggests that the known outlier sample has a particularly high EVOH content, in comparison to the calibration samples. Additional features in the residual spectrum that are not explained by the [EVOH − PA-6] spectrum might be due to the unique quality of the PE used in the outlier laminate sample.

Interpretation of the Calibration Models. Although the main goal of this work is to demonstrate the ability of the NIR method to determine selected quality parameters in food laminates, it is also important to identify possible interference effects that can arise in such NIR-laminate analyses. As described earlier, these interference effects can be studied by observation of the scores and loadings of the PCR models.

Laminate Study. For model interpretation purposes, only the model that uses the 1600–2240 nm region will be considered, because it is less complex and has a better prediction performance than the model that uses the 1500–2500 nm region. Table III indicates the percentage of variance in the spectral data that is explained by each principal component. These data indicate that the first principal component explains virtually all of the variation in the NIR data, and that the other three principal components explain rather weak effects.

In Fig. 6, the loading spectrum for the first principal component is compared to the subtraction spectrum of [PE − NEN]. The striking resemblance of these two spectra indicates that the first principal component predominantly explains the variation in the PE/NEN fraction (or PE%) in the laminates. This result (confirmed by observation of the PCR scores for principal component 1) is rather appealing, because it indicates that the most dominant variation in the NIR spectra is the most relevant to the prediction of PE%.

The second, third, and fourth principal components in the PCR model describe variations in the NIR spectra that are interferents to the determination of PE%. The loading spectrum for principal component 2 is compared to the mean of the calibration sample spectra in Fig. 7. This loading spectrum simply has positive bands of the laminate at shorter wavelengths (1600–2000 nm), and negative bands of the laminate at longer wavelengths (2000–2240 nm). Similar loading spectrum patterns, observed during an earlier PLS analysis of NIR spectra of polyurethanes,[23] was tentatively attributed to a variation in the wavelength-dependent scattering of the samples as a function of the scattering ability of the samples. It should also be noted that the scores for principal component 2 do not indicate any trend of this property with laminate composition or total thickness, but do indicate

TABLE III. Percentages of spectral variation described by each principal component: PE/NEN laminate spectra.

PC number	Percentage of spectral variation
1	93.5
2	5.8
3	0.5
4	0.1

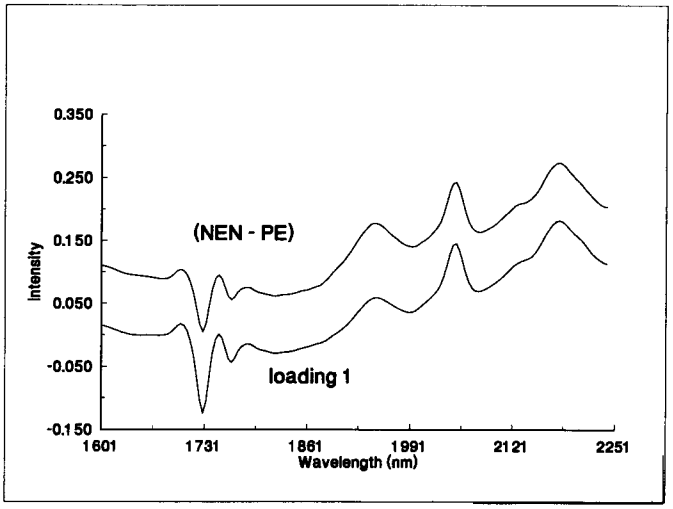

FIG. 6. Comparison of the loading spectrum for principal component 1 (obtained from the laminate spectra) with the subtraction spectrum of [pure NEN film − pure PE film]. The subtraction spectrum is scaled for clarity.

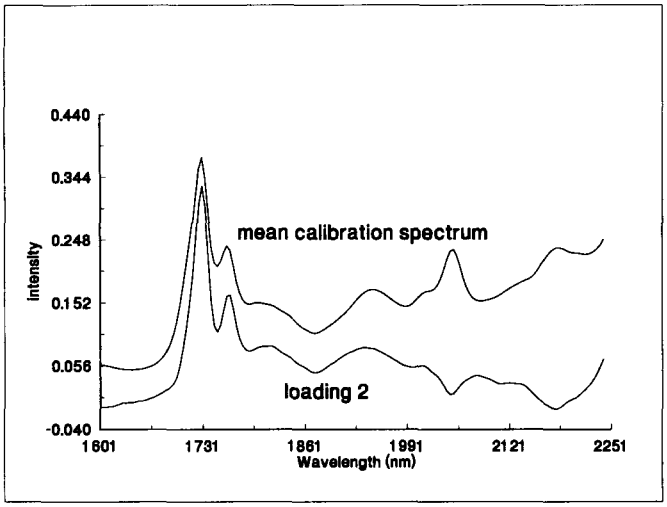

FIG. 7. Comparison of the loading spectrum for principal component 2 (obtained from the laminate spectra) with the mean calibration sample spectrum. The mean calibration spectrum is scaled for clarity.

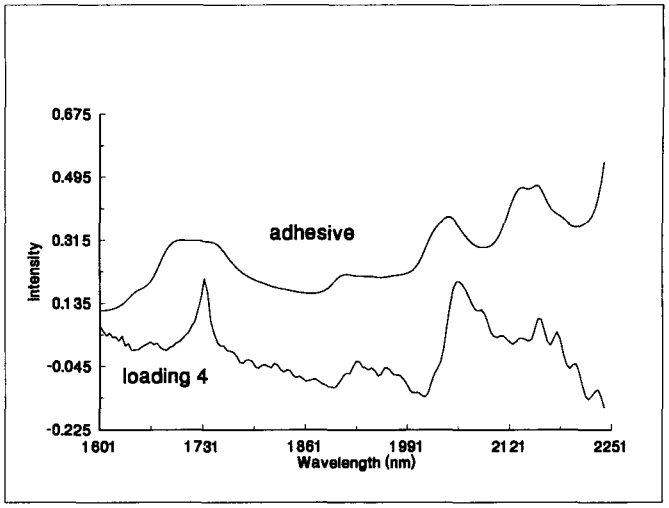

FIG. 9. Comparison of the loading spectrum for principal component 4 (obtained from the laminate spectra) with the spectrum of the polyurethane adhesive used in the laminates. The adhesive spectrum is scaled for clarity.

a small degree of clustering of the replicates for the different sample compositions. Therefore, this scattering-based variation might be caused by specular reflectance differences from nonreproducible placement of the laminate samples into the spectrometer, or from inherently different scattering properties of the different laminate compositions (from surface or interface roughness differences, or from differences in polymer morphology). Although this effect is considered an interferent in this case, it might be very useful for the analyses of highly scattering void- or particle-filled plastics,[23] in which the void or particle concentration is often a quantity of interest.

The loading spectrum for the third principal component is shown in Fig. 8. The most dominant feature in this loading spectrum, the strong positive peak at 1938 nm, is most probably an indication of variation in the amount of absorbed water in the PA-6 and EVOH parts

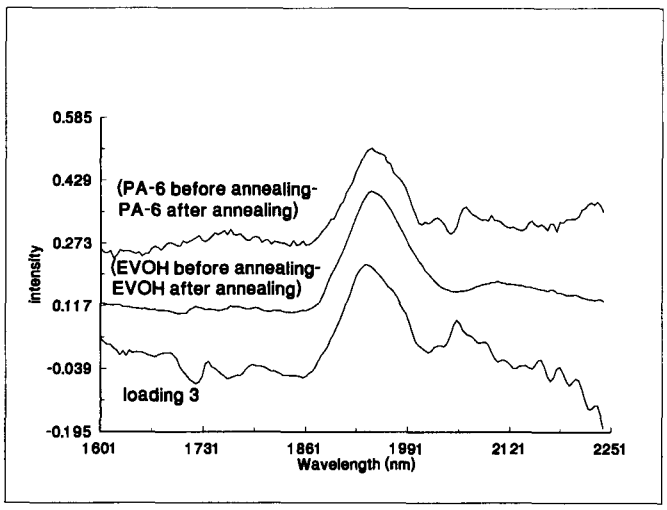

FIG. 8. Comparison of the loading spectrum for principal component 3 (obtained from the laminate spectra) with the subtraction spectra for both PA-6 and EVOH [before annealing − after annealing]. The subtraction spectra are scaled for clarity.

of the laminate. This conclusion is supported by comparison of this loading to the subtraction spectra of [EVOH before annealing − EVOH after annealing] and [PA-6 before annealing − PA-6 after annealing] (Fig. 8). The loss of water in these films, as a result of annealing, causes a decrease in an OH peak that is very close to the peak observed in the loading spectrum (as well as spectral shifts from morphological changes in the films). In addition, recent studies of relative humidity effects on the NIR spectrum of PA-6[24] revealed the presence of an OH combination band for bound water that is located at the same position as the band observed in the loading spectrum. The differing water contents of the laminates could have been caused by differing humidity histories of the films. However, the relative weakness of this principal component (0.5% of the variation in the NIR spectra) indicates that the water contents were rather well controlled in the laminate samples. Other weak features in the loading spectrum for the third principal component (in the regions 1700–1800 nm and 2000–2240 nm), might be caused by variations in the morphology of the PA-6, EVOH, or PE in the laminate, or by variations in the amount of polyurethane adhesive in the laminate. In particular, the features at 2000–2100 nm might correspond to shifts of NH and C=O bands as a result of hydrogen bonding with the absorbed water.

The loading spectrum for principal component 4, which explains only 0.1% of the variation in the NIR spectra, is shown in Fig. 9. The features in this loading spectrum are difficult to assign, because it was not possible to obtain very similar spectral features from the model compound spectra. However, some features in the range 2040 to 2240 nm in this loading resemble features in the spectrum of the polyurethane adhesive (also shown in Fig. 9). This observation leads one to suggest that this principal component, in part, describes a variation in the amount of polyurethane adhesive in the laminates.

NEN Study. Cross-validation analysis indicates the presence of two significant principal components of variation in the NEN film spectra. Observation of the scores

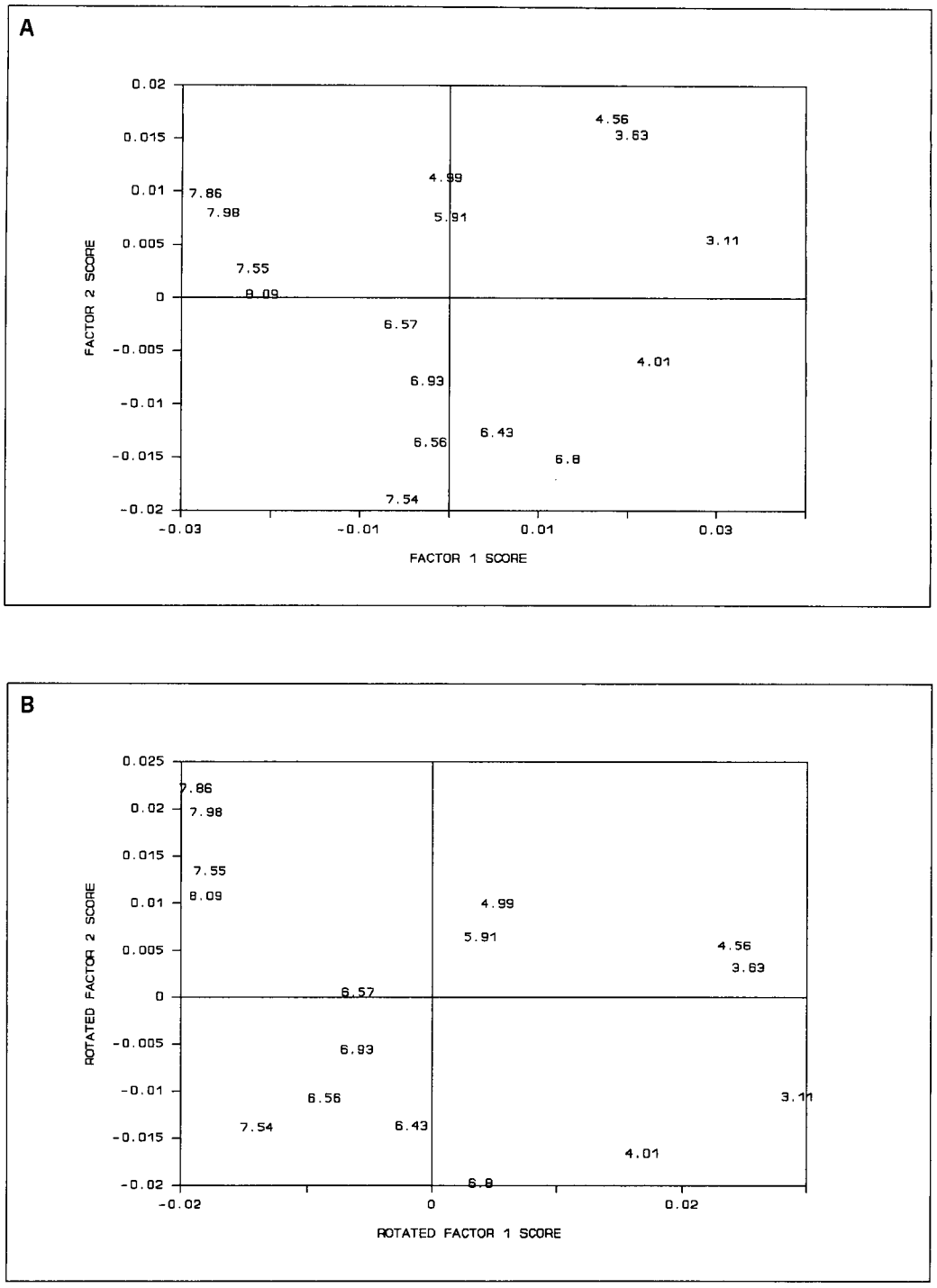

FIG. 10. Scores of the first and second principal components obtained from PCR analysis of the NIR spectra of NEN extrudates with different EVOH%: (**A**) as obtained from the PCR calibration; (**B**) after 30° rotation of the PCR principal components. Sample labels indicate EVOH%.

for these two principal components (Fig. 10A) indicates that the samples are well separated according to their EVOH%, but do not appear to follow a linear trend along a single principal component axis. Rotation of the PCR model by $\theta = 30°$ (according to Eqs. 5 and 6) results in a visual pattern of scores in which rotated component 1 corresponds more closely to the trend in the EVOH% (Fig. 10B). Although the optimal rotation angle could have been obtained by more mathematical means, the visually optimized procedure used here produced satisfactory results. After this rotation, components 1 and 2 describe 57.6% and 37.5% of the spectral variation, respectively.

The fact that rotated component 1 describes the variation in the EVOH% is supported by observation of the loading for this component (Fig. 11), which is very similar to the subtraction spectrum of [pure PA-6 − pure EVOH]. This result indicates that the NIR method is indeed sensitive to the EVOH%, rather than to another property that is by chance correlated to the EVOH%.

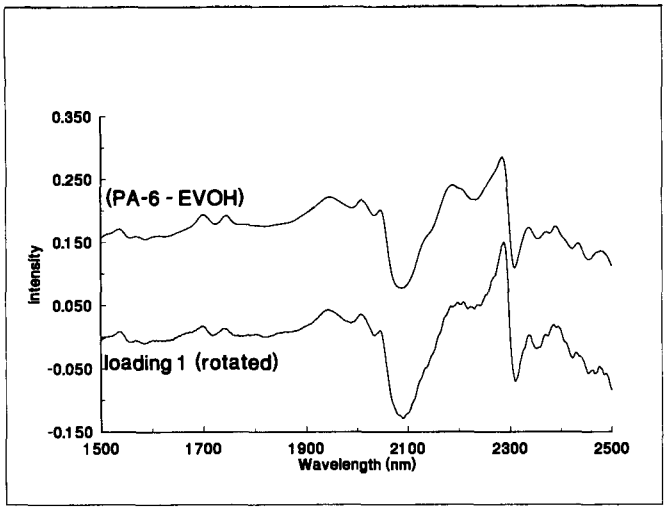

FIG. 11. Comparison of the loading spectrum for principal component 1 (obtained from the NEN spectra) with the subtraction spectrum of [pure PA-6 − pure EVOH]. The subtraction spectrum is scaled for clarity.

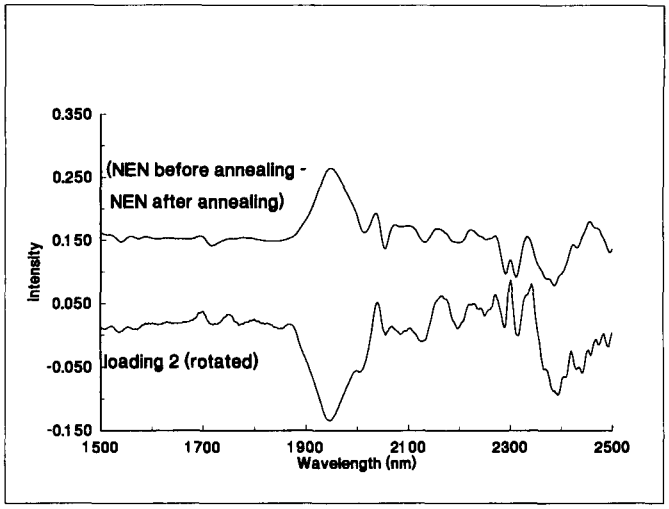

FIG. 12. Comparison of the loading spectrum for principal component 2 (obtained from the NEN spectra) with the subtraction spectrum of [NEN before annealing − NEN after annealing]. The subtraction spectrum is scaled for clarity.

The source of the second, less-relevant, source of variation in the NEN spectra is revealed by observation of the loading spectrum for rotated component 2 (Fig. 12). This loading, which is largely affected by the water band at 1946 nm, suggests the presence of significant variations in the amount of absorbed water in the samples. However, the trend in this loading spectrum from 2000 to 2500 nm is somewhat similar to the subtraction spectrum of [NEN before annealing − NEN after annealing] (also in Fig. 12). This result suggests that significant morphological variations of the PA-6 and EVOH layers are also present in the NEN samples.

To summarize, the NIR method appears to be sensitive to three properties that vary in the NEN samples: EVOH%, absorbed water content, and crystallinity or orientation of the PA-6 or EVOH. The fact that only two sources of variation were detected by cross-validation could be the result of a strong correlation between two of these three varying properties in the samples. The most likely possibility is that the absorbed water content is inversely related to the crystallinity or orientation of the PA-6 in the NEN samples. Because the humidity histories of the samples were very similar, such a relationship is expected, because increased crystallinity in the PA-6 would not only reduce the number of absorption sites for water in the film but also decrease the ability of water to penetrate the PA-6 layer and be absorbed by the EVOH layer.

CONCLUSIONS

These results indicate that the NIR reflective transmission method, combined with multivariate analysis techniques, can be used to determine the total thickness of a polyethylene/polyamide-6/EVOH laminate and the polyethylene thickness percentage in such laminates. Despite the practical limitations of the design of the laminate samples used in this work, our studies indicate that the NIR method has sufficient sensitivity to determine these properties. In addition, it was found that the NIR method can be used to determine the EVOH thickness in co-extruded NEN films within 0.7 to 0.8 μm. It should be noted that the results of this work are only directly applicable to PE/PA-6/EVOH laminates, but might have some relevance to the analyses of similar laminates.

This work also demonstrated that the PCR method, when used for calibration of NIR data, can also be used to (1) identify and partially characterize "outlier" prediction samples that are not appropriate for use with the PCR calibration, and (2) identify sources of interference in the NIR determinations. Through such interference analyses, it was found that the NIR method is sensitive to the absorbed water content, the morphology of the polyamide and/or EVOH, and possibly the amount of polyurethane adhesive in the laminates.

This study also revealed several "warnings" regarding the use of NIR spectroscopy for laminate analysis. First of all, it was found that scatter or reflection variations, probably produced from nonreproducible placement of samples into the spectrometer, can cause significant wavelength-dependent effects in the NIR spectra that cannot be filtered away by simple total thickness normalization and baseline correction. These effects could, in some cases, be larger than the spectral effect that is correlated to the property of interest. Therefore, it would be advantageous to sample as reproducibly as possible to minimize the prediction error. Second, the thickness of the laminate must be considered before an NIR calibration model is constructed. The use of laminates that are too thick (greater than approximately 250 μm for true transmission sampling) might result in nonlinearity for the $-CH_2-$ polyethylene bands at 2310 and 2350 nm. However, film samples that are very thin (approximately 25 to 50 μm) can produce significant interference fringe patterns in transmission spectra, depending on the surface roughness and optical transparency of the films. The variations from such fringes can dominate the NIR spectral variations and thus result in poor prediction results. In this case, optical interference fringe suppression methods could be used to produce better results.

ACKNOWLEDGMENTS

The author gratefully acknowledges Otto Nielsen Emballage AS (Lyngby, Denmark), and specifically Mr. E. Henningsen, for providing the samples used in this work. This research was supported by a fellowship sponsored by the Royal Norwegian Council for Scientific and Industrial Research.

1. J. Stepek, V. Duchacek, D. Curda, J. Horacek, and M. Sipek, *Polymers as Materials for Packaging* (Ellis Horwood Ltd., Chichester, 1987).
2. F. A. Paine, and H. Y. Paine, *A Handbook of Food Packaging* (Leonard Hill, Glasgow, 1983), pp. 36–53.
3. M. Mathlouthi, *Food Packaging and Preservation* (Elsevier, London, 1986).
4. J. Nentwig, Packaging (UK) **62,** 13 (1991).
5. J. Perdikoulias and W. Wybenga, Tappi J. **72(11),** 107 (1989).
6. C. E. Miller, Appl. Spectrosc. Rev. **26,** 275 (1991).
7. A. M. C. Davies, A. Grant, G. M. Gavrel, and R. V. Steeper, Analyst **110,** 643 (1985).
8. H. W. Siesler, Lanbauforsch. Völkenrode **107,** 112 (1989).
9. C. M. Paralucz, Appl. Spectrosc. **43,** 1273 (1989).
10. J. Nielsen, Emballering **4,** 51 (1984).
11. H. Martens and T. Næs, *Multivariate Calibration* (Wiley, Chichester, 1989), pp. 97–116.
12. W. Windig and H. L. C. Meuzelaar, in *Computer Enhanced Analytical Spectroscopy,* H. L. C. Meuzelaar and T. L. Isenhour, Eds. (Plenum, New York, 1987), pp. 81, 82.
13. W. Windig, J. Haverkamp, and P. G. Kistemaker, Anal. Chem. **55,** 81 (1983).
14. P. Geladi, D. MacDougall, and H. Martens, Appl. Spectrosc. **39,** 491 (1985).
15. J. L. Ilari, H. Martens, and T. Isaksson, Appl. Spectrosc. **42,** 722 (1988).
16. C. E. Miller and T. Næs, Appl. Spectrosc. **44,** 895 (1990).
17. H. Martens and E. Stark, J. Pharm. Biomed. Anal. **9,** 625 (1991).
18. H. Martens and T. Næs, *Multivariate Calibration* (Wiley, Chichester, 1989), pp. 250–58.
19. H. Martens and T. Næs, *Multivariate Calibration* (Wiley, Chichester, 1989), pp. 284–85.
20. H. Martens and T. Næs, *Multivariate Calibration* (Wiley, Chichester, 1989), pp. 116–146.
21. R. F. Edgar and B. J. Stay, *Infrared Technology and Applications,* SPIE Vol. 590 (SPIE, Bellingham, Washington, 1985), p. 316.
22. R. F. Edgar and P. H. Hindle, Proc. 4th Intl. Conf. on Near-infrared Spec., in press (1992).
23. C. E. Miller and B. E. Eichinger, J. Appl. Poly. Sci. **42,** 2169 (1991).
24. M. Fukuda, M. Miyagawa, H. Kawai, N. Yagi, O. Kimura, and T. Ohta, Polym. J. **19,** 785 (1987).